2024 IEEE International Conference on Robotics and Automation (ICRA 2024)
May 13-17, 2024. Yokohama, Japan

Highway-Driving with Safe Velocity Bounds on Occluded Traffic

Truls Nyberg*[1], Jonne van Haastregt*, and Jana Tumova

***Abstract*— Limited visibility and sensor occlusions pose pressing safety challenges for advanced driver-assistance systems (ADAS) and autonomous vehicles (AVs). In this work, our pursuit was to strike a balance: a method that ensures safety in occluded scenarios while preventing overly cautious behavior. We argue that such approaches are crucial for AVs' future, particularly when navigating alongside human drivers on highways at high speeds. To this end, we used reachability analysis to find safe velocity bounds on occluded traffic participants. Compared to state-of-the-art methods, we achieved velocity increases in more than 60% of the 230 cut-in scenarios from the highD dataset, without sacrificing safety.**

I. Introduction

Most new vehicles today are equipped with Automatic Emergency Braking systems (AEB). These systems are designed to detect objects in front of the vehicle and brake sufficiently when a collision threat emerges [1], [2]. Yet, current AEB systems struggle with objects that suddenly appear in their sensor view. A stationary vehicle may be hiding behind the next crest, or behind a lane-changing truck, as illustrated in Fig. 1. In these scenarios, the human driver is expected to intervene in order to prevent a collision.

Recently, systems with higher levels of automation have emerged, like Mercedes's Drive Pilot [3], and robotaxi services from Waymo and Cruise [4]. Despite these advancements, the degree of required safety remains a topic of debate [5]. Several frameworks have been proposed for the design, verification, and validation of Autonomous Vehicles (AVs) [6], and formalization of adherence to road rules [7]–[13].

Despite numerous proposed occlusion-aware methods, none have yet formally tackled the dual challenge of 1) ensuring safety on highways by anticipating occluded stationary vehicles while 2) avoiding excessive caution in the face of new occlusions. For instance, in Fig. 1, the red vehicle must take into account the possibility of a stationary vehicle in its lane hiding behind the truck. However, despite the occlusion, the yellow vehicle has prior knowledge that there is no stationary vehicle in *its* lane. It only has to keep a safe distance to the moving truck.

In this paper, we present a novel solution that builds on state-of-the-art formal methods and mitigates the limitations of statistical or learning-based methods in these critical events that are sparsely presented in data.

[1]The author is employed by Scania CV AB, 151 87 Södertalje, Sweden.
*The authors contributed equally to this work. All authors are affiliated with KTH Royal Institute of Technology, 100 44 Stockholm, Sweden. Email:{trulsny, jmvh, tumova}@kth.se. The work was partially supported by the Wallenberg AI, Autonomous Systems and Software Program (WASP) funded by the Knut and Alice Wallenberg Foundation.

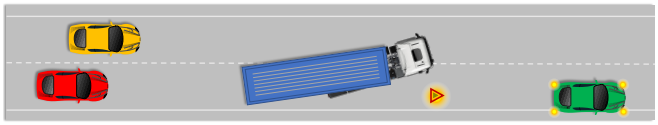

Fig. 1. The truck creates an occlusion. The red car needs to reduce its velocity sufficiently to stop for the stationary green car. Meanwhile, the yellow car only needs to adjust its speed for the cut-in, as it previously saw that its lane was clear of stationary objects.

A. Related Work

Data-driven methods excel at predicting likely traffic behaviors [14], even surpassing human performance [15]. Yet, they struggle when forecasting rare (but potentially legal) behaviors, such as sudden braking for an occluded vehicle ahead. To address this, model-based formal methods, such as set-based predictions, can be utilized [16]. In [17], the authors enhance these methods to also predict occluded traffic by considering *virtual objects* outside a vehicle's sensor view, similar to [18] and [19]. If available, Vehicle-to-Everything (V2X) communication can also be used to enhance a vehicle's perception beyond its limits [20]–[23].

Once traffic is predicted, a safe, efficient, and comfortable trajectory should be planned [24]. Often, safety and efficiency objectives are conflicting, and risk-aware trade-offs must be made [25]–[27]. Many recent works have delved into risk-aware approaches for planning in the presence of occlusions [28]–[33]. Information gathering can also explicitly be added as an objective to help maximize a vehicle's viewpoints [34], [35]. The challenge of occlusion-aware planning can also be formulated as a Partially Observable Markov Decision Process [36]–[38]. Game theory [39], [40] and data-driven techniques [41], [42] have also been explored.

A different approach for dealing with occlusions and thus enhancing planning performance is to reason about what states the occluded vehicles may be in. The occluded area may change rapidly, especially when it is caused by dynamic obstacles close to a sensor's viewpoint. By using previous observations, and assumptions on how occluded objects may move, virtual objects in impossible positions can be removed [43]–[45]. In [46], the authors also present a method for upper-bounding velocities of possible vehicles in occluded positions at lane centerlines, yielding improved performance in occluded urban intersections.

B. Contribution

In this work, we extend our method in [43] to track and establish upper and lower bounds of the velocities of vehicles in occlusions. Through efficient modeling, we provide real-time safety guarantees without restricting the shape of the possible objects. We believe this advancement is pivotal for

ensuring safety and efficiency, especially in highway driving, as further demonstrated in our evaluation section.

II. Problem Formulation

A. Notation

We denote scalars with lowercase letters, e.g., a; vectors with bold lowercase letters, e.g., $\mathbf{a}$; matrices with bold capital letters, e.g., $\mathbf{A}$; and sets with calligraphy capital letters, e.g., $\mathcal{A}$. Additionally, we indicate an over-approximation with a hat, e.g., $\hat{\mathcal{A}} \supseteq \mathcal{A}$. States, state vectors, or sets of states over continuous time are denoted with the time in parenthesis, e.g., $\mathbf{A}(t)$; and we use subscripts to refer to a specific time τ, e.g., $\mathbf{a}_\tau$, where $\tau \geq 0$ is the time elapsed from an initial time $\tau_0 = 0$. Closed continuous intervals are denoted as $[\underline{a}, \overline{a}]$, ranging from the lower bound $\underline{a}$ to the upper bound $\overline{a}$. The symbol $\oplus$ is used for the Minkowski sum, the function $\mathrm{conv}(\mathcal{A})$ takes the convex hull of the set $\mathcal{A}$, and $\mathrm{proj}_{\square}(\mathcal{A})$ projects the set $\mathcal{A}$ onto the dimensions in $\square$ (e.g., xy).

B. Set-based Model of a Traffic Scenario

We consider a set of traffic participants, including an ego vehicle and other traffic participants. A traffic participant at time t is represented as a set of states $\mathcal{X}(t) \subset \mathbb{R}^n$.

Definition 1 (Model M)**.** Each traffic participant is modeled as $M := \langle \mathbf{f}^M, \mathcal{X}^M, \mathcal{U}^M \rangle$, where $\dot{\mathbf{x}}(t) = \mathbf{f}^M(\mathbf{x}(t), \mathbf{u}(t))$ describes the state dynamics, $\mathcal{X}^M \subseteq \mathbb{R}^n$ denotes the admissible set of states, and $\mathcal{U}^M \subseteq \mathbb{R}^m$ the admissible set of inputs.

The notion of occupied space and field of view below are given from the ego vehicle's perspective.

Definition 2 (Occupied space, $\mathcal{O}(t)$)**.** The occupied space is the set of points in the xy-plane occupied by other traffic participants, namely $\mathcal{O}(t) = \mathrm{proj}_{xy}(\mathcal{X}^o(t))$, where $\mathcal{X}^o(t)$ is the set of all other traffic participants' states at time t.

Definition 3 (Field of View, $\mathcal{F}(t)$)**.** The field of view is the set of points on the xy-plane, $\mathcal{F}(t) \subset \mathbb{R}^2$, within direct line of sight of a vehicle's sensors, and within the sensors' range.

To represent that the traffic participants should only be occupying space in the legally drivable area and obey various rules, we introduce the notion of valid states.

Definition 4 (Valid states, $\mathcal{X}^{valid}$)**.** The set of valid states for a traffic participant is

$$\mathcal{X}^{valid} = \{\mathbf{x} \in \mathbb{R}^n \mid \mathrm{proj}_{xy}(\mathbf{x}) \in \mathcal{L} \wedge \mathbf{x} \in \mathcal{C}\},$$

where $\mathcal{L} \subseteq \mathbb{R}^2$ is the legal drivable area and $\mathcal{C} \subseteq \mathbb{R}^n$ are constraints (e.g., a heading constraint c_φ or a speed limit c_v).

C. Trajectory planning problem

We are interested in planning feasible collision-free trajectories for the ego vehicle. We consider online planning in which a new trajectory is planned based on the latest sensor information in a receding horizon fashion. The planned trajectories are represented with N future states with a discrete time step of Δt, where each state corresponds to a fixed point of the ego vehicle (e.g., the center point of the vehicle). For simplicity, we assume a constant planning frequency of $1/\Delta t$. Before formally defining a *feasible* and *collision-free* trajectory, we introduce reachable sets.

Definition 5 (Reachable set, $\mathcal{R}$)**.** Given a model M and a set of states $\mathcal{X}_\tau \subseteq \mathcal{X}^M$ at time τ, $\mathcal{R}(M, \mathcal{X}_\tau, \Delta t)$ denotes the set of states reachable from $\mathcal{X}_\tau$ exactly at time $\tau + \Delta t$:

$$\mathcal{R}(M, \mathcal{X}_\tau, \Delta t) = \Big\{ \mathbf{x}(\tau) + \int_\tau^{\tau+\Delta t} \mathbf{f}^M(\mathbf{x}(t), \mathbf{u}(t)) dt \;\Big|\; \mathbf{x}(\tau) \in \mathcal{X}_\tau,\, \mathbf{x}(t) \in \mathcal{X}^M,\, \mathbf{u}(t) \in \mathcal{U}^M \;\forall t \in [\tau, \tau + \Delta t] \Big\}.$$

For an interval $[t_a, t_b]$ where $\tau \leq t_a < t_b$,

$$\mathcal{R}(M, \mathcal{X}_\tau, [t_a, t_b]) = \bigcup_{t_a \leq t \leq t_b} \mathcal{R}(M, \mathcal{X}_\tau, t - \tau).$$

Definition 6 (Feasible trajectory)**.** A feasible trajectory T (under a model M) is a sequence of N states from some initial state at time τ, denoted x_τ, to a final state $x_{\tau+N\Delta t}$, such that $T := \langle \mathbf{x}_\tau, \mathbf{x}_{\tau+\Delta t}, \mathbf{x}_{\tau+2\Delta t}, ..., \mathbf{x}_{\tau+N\Delta t} \rangle$, where $\mathbf{x}_{\tau+i\Delta t} \in \mathcal{R}(M, \mathbf{x}_{\tau+(i-1)\Delta t}, \Delta t), \forall i \in [1, \ldots, N]$.

Definition 7 (Collision-free trajectory)**.** For a traffic participant with an initial set of states $\mathcal{X}_\tau \notin \mathcal{X}^o_\tau$, its trajectory, T_{safe}, is *collision-free* if $\mathcal{X}(t) \notin \mathcal{O}(t), \forall t \in [\tau, \tau + N\Delta t]$.

Ultimately, we aim to find the best feasible trajectory that is *guaranteed* to be collision-free. Hence, it is important that the prediction of other traffic participants is conservative, yet not overly conservative.

Problem 1 (The Planning Problem)**.** Given a Field of View, $\mathcal{F}_\tau$, a model for the ego vehicle, M_{ego}, and a model for other traffic participants, M_{other}, find the best feasible trajectory T (given a cost function) that is guaranteed to be collision-free.

Problem 2 (The Prediction Problem)**.** Given a Field of View, $\mathcal{F}_\tau$, and a model of other traffic participants, M_{other}, find the set of states for possible (including possibly hidden) traffic participants that minimally over-approximate the occupied space at future time.

III. Method

A. Reachability Computations

We assume that all traffic participants such as cars, trucks, and motorcycles can be modeled accurately using the nonlinear bicycle model [47], $M_{bic} \coloneqq \langle \mathbf{f}^{bic}, \mathcal{X}^{bic}, \mathcal{U}^{bic} \rangle$, where

$$\mathbf{f}^{bic} \coloneqq \begin{cases} \dot{x}(t) = v(t)\cos(\varphi(t)), \\ \dot{y}(t) = v(t)\sin(\varphi(t)), \\ \dot{\varphi}(t) = v(t)\tan(\theta(t))/L, \\ \dot{v}(t) = a(t), \end{cases}$$

$$\mathcal{X}^{bic} \coloneqq \mathcal{X}^{valid},$$

$$\mathcal{U}^{bic} \coloneqq \{\theta \in [-c_\theta, c_\theta],\ a \in [c_{a,min}, c_{a,max}]\}.$$

The model has states x, y, an orientation φ, and a velocity v. The length between the front and rear axle, the wheelbase, is denoted L. As inputs, the model takes a steering angle θ

and an acceleration a. The constraints $c_{a,min}$, $c_{a,max}$, and c_θ, should be over-approximated such that the model can surely represent all motions that the autonomous ego vehicle could expect from other traffic participants. In this work, the x-coordinate is assumed to be aligned with the driving direction of the ego vehicle's lane, and the headings of all other traffic participants are assumed to be in $[-c_\varphi, c_\varphi]$ with $c_\varphi \leq \pi/2$ during the relevant time horizon.

The reachable set of the non-linear bicycle model is difficult to compute or directly over-approximate [48]. However, reachable sets can be computed for several linear model abstractions and then combined. If each abstraction yields an over-approximation of the original reachable set, the intersection of the abstraction's reachable sets is also an over-approximation [17].

Lemma 1. For a model M, where $\mathcal{X}^M = \mathbb{R}^n$, and $\mathbf{f}^M$ is a continuous linear time-invariant system, the reachable set for any $\Delta t > 0$ can be over-approximated as

$$\hat{\mathcal{R}}(M, \mathcal{X}_\tau, \Delta t) = e^{\mathbf{A}\Delta t}\mathcal{X}_\tau \oplus \sum_{i=0}^{\infty} \frac{\mathbf{A}^i \Delta t^{i+1}}{(i+1)!}\mathcal{U}^M, \quad (1)$$

where $e^{\mathbf{A}\Delta t}\mathcal{X}_\tau = (\mathbf{I} + \mathbf{A}\Delta t + \mathbf{A}^2\Delta t^2/2! + \ldots)\mathcal{X}_\tau$.

Proof (Sketch). We refer the reader to [48, ch. 3.2]. The above equation is achieved when adding the system's homogeneous and inhomogeneous solutions together and considering infinitely many terms in the sum. □

In this work, we will combine a model abstraction, M_{vel}, that over-approximate the reachable set of states in (x, y), with a model abstraction, M_{acc}, that over-approximate the reachable set of states in (x, v).

The first abstraction, $M_{vel} := \langle \mathbf{f}^{vel}, \mathcal{X}^{vel}, \mathcal{U}^{vel} \rangle$, is a simple single integrator model, where

$$\begin{aligned}
\mathbf{f}^{vel} &:= \begin{cases} \dot{x}(t) = v_x(t), \\ \dot{y}(t) = v_y(t), \end{cases} \\
\mathcal{X}^{vel} &:= \{(x, y) \in \mathbb{R}^2\}, \\
\mathcal{U}^{vel} &:= \{(v_x, v_y) \mid \sqrt{v_x^2 + v_y^2} < c_{v,max} \\
&\qquad \wedge\ |\mathrm{atan2}(v_y, v_x)| < c_\varphi\}.
\end{aligned}$$

This model is linear and only has two states, x and y, and two inputs, v_x and v_y. Since the states are directly controlled by the input, the system matrix is $\mathbf{A}_{vel} = \mathbf{0}$.

Lemma 2. A traffic participant occupying any space in the set $\mathrm{proj}_{xy}(\mathcal{X}_\tau) \subseteq \mathrm{proj}_{xy}(\mathcal{X}^{valid})$ at any time τ is bound to at a future time $\tau + \Delta t$ only occupy space in

$$\mathrm{proj}_{xy}(\mathcal{R}(M_{bic}, \mathcal{X}_\tau, \Delta t)) \subseteq \hat{\mathcal{R}}(M_{vel}, \mathrm{proj}_{xy}(\mathcal{X}_\tau), \Delta t).$$

Proof (Sketch). The reachable set of the single integrator is a circle segment and the reachable positions of the bicycle model are within a cone shape with concave arcs as sides. Using trigonometry, the over-approximation can be shown. □

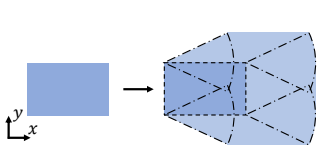

Fig. 2. Reachability of a set $\mathcal{X}_t$ using the model M_{vel}.

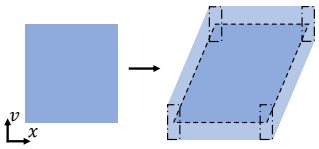

Fig. 3. Reachability of a set $\mathcal{X}_t$ using the model M_{acc}.

Similarly, we now consider the second model abstraction $M_{acc} := \langle \mathbf{f}^{acc}, \mathcal{X}^{acc}, \mathcal{U}^{acc} \rangle$, where

$$\begin{aligned}
\mathbf{f}^{acc} &:= \dot{x}(t) = v(t), \\
&\qquad \dot{v}(t) = a_x(t), \\
\mathcal{X}^{acc} &:= \{[x, v] \in \mathbb{R}^2\}, \\
\mathcal{U}^{acc} &:= \{a_x \mid c_{a,min}/\cos(c_\varphi) \leq a_x \leq c_{a,max}\}.
\end{aligned}$$

This model describes traffic participants' dynamics along the x-axis as a double integrator system. It has two states, x and v, and one input, a_x. The minimal acceleration in x is $c_{a,min}/\cos(c_\varphi)$, where c_φ is the heading constraint. Being linear and time-invariant, we can represent the model in the state-space form $\dot{\mathbf{x}}(t) = \mathbf{A}_{acc}\mathbf{x}(t) + \mathbf{u}(t)$, with

$$\mathbf{A}_{acc} = \begin{bmatrix} 0 & 1 \\ 0 & 0 \end{bmatrix}.$$

Lemma 3. The projection onto the xv-plane of a traffic participant's set of states reachable from some initial set of states $\mathcal{X}_\tau$ at a time τ, must at a future time $\tau + \Delta t$ be in

$$\mathrm{proj}_{xv}(\mathcal{R}(M_{bic}, \mathcal{X}_\tau, \Delta t)) \subseteq \hat{\mathcal{R}}(M_{acc}, \mathrm{proj}_{xv}(\mathcal{X}_\tau), \Delta t),$$

where $\hat{\mathcal{R}}(M_{acc}, \mathrm{proj}_{xv}(\mathcal{X}_\tau), \Delta t)$ over-approximates and bounds the velocities at corresponding positions along x.

Proof (Sketch). Since the bicycle model's reachable states in (x, v) are governed by the double integrator dynamics, the abstraction is simply a change of input from a to a_x. To translate the constraints on heading and velocity, we identify that the maximum reach in x is achieved with maximal acceleration and zero heading, and minimum reach is achieved with minimum acceleration and maximal heading. □

To over-approximate the reachable set from M_{vel}, we insert $\mathbf{A}_{vel} = \mathbf{0}$ in (1), yielding

$$\hat{\mathcal{R}}(M_{vel}, \mathcal{X}_\tau, \Delta t) = \mathcal{X}_\tau \oplus \Delta t\, \mathcal{U}^{vel},$$

since all higher powers $\mathbf{A}_{vel}^i = \mathbf{0}$. The reachable set is thus the initial set, Minkowski summed with the time-scaled input set. This set is visualized in Fig. 2.

For M_{acc}, we note that the system matrix is nilpotent with $\mathbf{A}_{acc}^2 = \mathbf{0}$, yielding the over-approximated reachable set

$$\hat{\mathcal{R}}(M_{acc}, \mathcal{X}_\tau, \Delta t) = \begin{bmatrix} 1 & \Delta t \\ 0 & 1 \end{bmatrix} \mathcal{X}_\tau \oplus \begin{bmatrix} \frac{1}{2}\Delta t^2 \\ \Delta t \end{bmatrix} \mathcal{U}^{acc}. \quad (2)$$

Equation (2) can be interpreted as skewing the initial set in x and Minkowski summing it with a time-scaled version of the input set. This interpretation is visualized in Fig. 3. The analytical solution to the reachable set of a double integrator

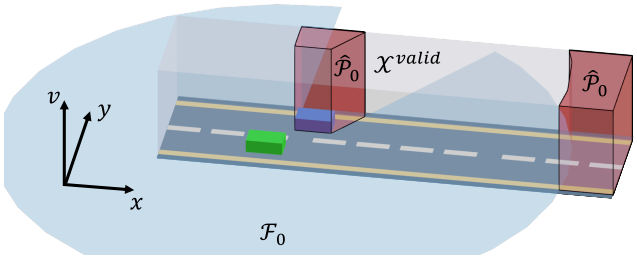

Fig. 4. Field of view, $\mathcal{F}_0$, in light blue, valid states, $\mathcal{X}^{valid}$, in grey, the possible set of states of others, $\hat{\mathcal{P}}_0$ in red. Green is ego, blue is others.

is found in [49]. With these insights, we can now combine the abstractions to over-approximate the original bicycle model.

Theorem 1. The reachable set of states at time $\tau + \Delta t$, for a traffic participant currently in the set of states $\mathcal{X}_\tau$, can be over-approximated such that

$$\mathcal{R}(M_{bic}, \mathcal{X}_\tau, \Delta t) \subseteq (\hat{\mathcal{R}}(M_{vel}, \text{proj}_{xy}(\mathcal{X}_\tau), \Delta t) \times \mathbb{R}_v \cap \mathcal{I}_{xyv}(\hat{\mathcal{R}}(M_{acc}, \text{proj}_{xv}(\mathcal{X}_\tau), \Delta t) \times \mathbb{R}_y)) \cap \mathcal{X}^{valid},$$

where we introduce the mapping $\mathcal{I}_{xyv} : (x, v, y) \mapsto (x, y, v)$ to correct the element order after the Cartesian products with the missing dimensions. We denote the over-approximated reachable set as $\hat{\mathcal{R}}(M_{bic}, \mathcal{X}_\tau, \Delta t)$.

Proof. This follows from Def 4 and Lemma 1, 2, 3. □

B. Tracking of Possible Traffic Participants' States

Definition 8 (Initial possible traffic participants' states, $\mathcal{P}_0$)**.** Given an initial field of view, $\mathcal{F}_0$, and a set of valid states, $\mathcal{X}^{valid}$, the initial possible traffic participants' states are

$$\hat{\mathcal{P}}_0 = \{\mathbf{x} \in \mathcal{X}^{valid} \mid \text{proj}_{xy}(\mathbf{x}) \notin \mathcal{F}_0\}.$$

Note that both the occupied space of a vehicle within the line of sight and the occluded space behind it is considered to be outside $\mathcal{F}_0$ and in the set $\hat{\mathcal{P}}_0$. An example of $\mathcal{F}_0$, the valid states $\mathcal{X}^{valid}$ and the resulting initial set of possible states of traffic participants $\hat{\mathcal{P}}_0$ are given in Fig. 4. At subsequent time steps, a possible traffic participant state must be outside the field of view at that time step and have been reachable from previous sets of possible participants' states.

Lemma 4. For all $i \in \mathbb{N}$, the set of states of all other traffic participants $\mathcal{X}^o_\tau$ at time $\tau = i\Delta t$ must be a subset of

$$\hat{\mathcal{P}}_\tau = \{\mathbf{x} \in \hat{\mathcal{R}}(M_{bic}, \hat{\mathcal{P}}_{\tau-\Delta t}, \Delta t) \mid \text{proj}_{xy}(\mathbf{x}) \notin \mathcal{F}_\tau\}.$$

Proof. This follows recursively from Theorem 1 and Def. 8. □

Algorithm 1 shows how this can be used to address Problem 2 and find safe velocity bounds on possible traffic participants. Given a field of view, $\mathcal{F}_\tau$, and the model of other traffic participants, M_{bic}, we reduce the possible other traffic participants' states that the planner has to consider.

Algorithm 1 Occlusion Tracking

Input: Previous set $\hat{\mathcal{P}}_{\tau-\Delta t}$, current field of view $\mathcal{F}_\tau$.
Output: Current set $\hat{\mathcal{P}}_\tau$.

if $\hat{\mathcal{P}}_{\tau-\Delta t} = \emptyset$ **then**
  return $\hat{\mathcal{P}}_\tau \leftarrow \mathcal{X}^{valid} - (\mathcal{F}_\tau \times \mathbb{R}_v)$ ▷ Initialise $\hat{\mathcal{P}}_0$
$\mathcal{X}_{vel} \leftarrow \text{proj}_{xy}(\hat{\mathcal{P}}_{\tau-\Delta t})$
$\mathcal{X}_{acc} \leftarrow \text{proj}_{xv}(\hat{\mathcal{P}}_{\tau-\Delta t})$
$\hat{\mathcal{R}}_{vel} \leftarrow (\mathcal{X}_{vel} \oplus \Delta t \mathcal{U}^{vel}) \times \mathbb{R}_v$
$\hat{\mathcal{R}}_{acc} \leftarrow \left(\begin{bmatrix} 1 & \Delta t \\ 0 & 1 \end{bmatrix} \mathcal{X}_{acc} \oplus \begin{bmatrix} \frac{1}{2}\Delta t^2 \\ \Delta t \end{bmatrix} \mathcal{U}^{acc} \right) \times \mathbb{R}_y$
$\hat{\mathcal{R}}_{bic} \leftarrow \hat{\mathcal{R}}_{vel} \cap \left(\mathcal{I}_{xyv} \left(\hat{\mathcal{R}}_{acc} \right) \right) \cap \mathcal{X}^{valid}$
return $\hat{\mathcal{P}}_\tau \leftarrow \hat{\mathcal{R}}_{bic} - (\mathcal{F}_\tau \times \mathbb{R}_v)$

Algorithm 2 Occlusion-aware Trajectory Planning

Input: Current set $\hat{\mathcal{P}}_\tau$, current ego states, $\mathcal{X}^{ego}_\tau$,.
Output: Planned trajectory, $T = \langle \mathbf{x}_{\tau+\Delta t}, ..., \mathbf{x}_{\tau+N\Delta t} \rangle$.

for $\ell \leftarrow 1$ to L **do** ▷ For each lane
  $\mathcal{X}^{valid} \leftarrow \{\mathbf{x} \in \mathbb{R}^n \mid \text{proj}_{xy}(\mathbf{x}) \in \mathcal{L}^\ell \wedge \mathbf{x} \in \mathcal{C}\}$
  for $i \leftarrow 1$ to N **do** ▷ Predict occupied space
    $t_b \leftarrow \tau + i\Delta t$
    $t_a \leftarrow t_b - \Delta t$
    $\hat{\mathcal{O}}^\ell_{[t_a,t_b]} \leftarrow \text{proj}_{xy}(\hat{\mathcal{R}}(M_{bic}, \hat{\mathcal{P}}_\tau, [t_a, t_b]))$
    $\hat{\mathcal{O}}_{[t_a,t_b]} \leftarrow \hat{\mathcal{O}}_{[t_a,t_b]} \cup \hat{\mathcal{O}}^\ell_{[t_a,t_b]}$
$\mathcal{T} = \text{generateTrajectories}(\mathcal{X}^{ego}_\tau)$
$\mathcal{T}_s = \text{getSafeTrajectories}(\mathcal{T}, \langle \hat{\mathcal{O}}_{[\tau,\tau+\Delta t]}, \ldots, \hat{\mathcal{O}}_{[t_a,t_b]} \rangle)$
$T = \text{getBestTrajectory}(\mathcal{T}_s)$
return T

C. Occlusion-Aware Trajectory Planning

We also use reachability analysis to predict the possible traffic participants' states at *future* time steps in our planned trajectory. To guarantee that our planned trajectory is collision-free *in between* two consecutive time steps, the reachable set must be computed for the N time *intervals* between each state in the planned trajectory.

From [48] we know that Lemma 1 extends to

$$\hat{\mathcal{R}}(\mathcal{X}_0, [\underline{t}, \bar{t}]) = \text{conv}(e^{\mathbf{A}\underline{t}}\mathcal{X}_0 \cup e^{\mathbf{A}\bar{t}}\mathcal{X}_0) \oplus \sum_{i=0}^{\infty} \frac{\mathbf{A}^i \bar{t}^{i+1}}{(i+1)!} \mathcal{U}^M.$$

The over-approximated reachable set in Theorem 1 can thus also be computed over time intervals. These reachable sets can then be projected on the xy-plane to find the space that may be occupied during the time intervals.

Definition 9 (Predicted occupied space $\hat{\mathcal{O}}$)**.** The predicted occupied space, $\hat{\mathcal{O}}_{[t_a,t_b]}$, is the space in xy that may be occupied by (possibly hidden) traffic participants during the time interval $[t_a, t_b]$, given a set of possible traffic participant states, $\hat{\mathcal{P}}_\tau$, at a time $\tau \leq t_a < t_b$. It can be computed as

$$\hat{\mathcal{O}}_{[t_a,t_b]} = \text{proj}_{xy}(\hat{\mathcal{R}}(M_{bic}, \hat{\mathcal{P}}_\tau, [t_a, t_b])).$$

In Algorithm 2, we show how to plan with the predicted occupancies, effectively solving Problem 1. As the input,

the algorithm takes the current set of ego states, $\mathcal{X}_\tau^{ego}$, together with the tracked set of possible traffic participants' states, $\hat{\mathcal{P}}_\tau$, from Algorithm 1. We assume that the other traffic participants are responsible in the following sense: they ensure a safe distance to others when changing lanes or approaching vehicles from behind. This allows us to focus on predicting possible traffic participants per lane, ahead of the ego vehicle.

As the output, the algorithm produces the best collision-free trajectory, T, given a cost function. The methods $\mathrm{generateTrajectories}$, $\mathrm{getSafeTrajectories}$, and $\mathrm{getBestTrajectory}$ generate candidate trajectories, filter out collision-free trajectories, and return the best trajectory.

IV. Evaluation

A. Experiments Setup

We demonstrate the use of finding safe velocity bounds on occluded traffic in a highway setting where the ego vehicle gets overtaken. Such scenarios highlight the need for also *lower* bounding the possible velocities in occlusions. The goal here, given through a cost function, is to stay in the middle of a lane and keep the velocity close to a target speed, while ensuring a safe distance to possible traffic participants ahead. We consider the distance safe when the ego vehicle can find a collision-free trajectory, assuming a maximum deceleration of all other (possibly hidden) traffic participants. To investigate the efficacy of our implemented solution, we measure the ego vehicle's maximal deviation from the target speed (i.e., the speed reduction) in a set of recorded highway scenarios. A range sensor is assumed to provide a field of view for the ego vehicle.

1) Implementation Details: The highD dataset [50] is used to supply real traffic scenarios. To simulate, visualize, and interact with the scenarios, we use the CommonRoad toolbox [51]. All the sets of states are represented as collections of polygons or polyhedra using the C++ library CGAL [52]. The library provides functions for the operations needed, e.g., intersection, Minkowski sum, convex hull, etc.

To implement Algorithm 1, we create a polygon for the field of view, $\mathcal{F}_\tau$, by ray tracing from the ego vehicle in small angular steps, either to the sensor's max range or to other vehicles in the scenario. The algorithm's output, the set of possible states of other traffic participants, $\hat{\mathcal{P}}_\tau$, is fed as input to Algorithm 2 and to itself for the next time step.

Algorithm 2 is inspired by our previous work [43] and uses a simple planner that only samples trajectories with the maximal, minimal, or zero acceleration input along the centerline of a lane. The main difference from [43] is that CGAL is used for the reachability and occupancy computations. The resulting sets of occupancy (line 6) are converted to Shapely polygons [53] to use in the drivability-checker from CommonRoad [54]. All the parameters used are shown in Table I. The code is also available at github.com/haastregt/occlusion_tracking.

2) Baseline Method: We compare with our previous approach for occlusion tracking from [43], which we showed to be similar in performance to other state-of-the-art methods, such as [45] and [44]. The baseline method is implemented by just removing $\hat{\mathcal{R}}_{acc}$ in Algorithm 1 and Algorithm 2 when over-approximating $\hat{\mathcal{R}}_{bic}$. This means that the possibly occupied space will be tracked, but not which velocities traffic participants may have at these positions.

TABLE I
Parameters used during simulations on the highD dataset

Others' Parameters			Ego's Parameters		
c_φ	10	$^\circ$	N	$\max(30, \lceil \frac{v_{ref}}{a_{min}\Delta t} \rceil)$	
$c_{v,min}$	0	$\mathrm{km\,h^{-1}}$	Range	250	m
$c_{v,max}$	135	$\mathrm{km\,h^{-1}}$	Δt	0.2	s
$c_{a,min}$	-5	$\mathrm{m\,s^{-2}}$	a_{min}	-5	$\mathrm{m\,s^{-2}}$
$c_{a,max}$	3	$\mathrm{m\,s^{-2}}$	a_{max}	3	$\mathrm{m\,s^{-2}}$

3) Scenario Filtering: To study the effect of tracking velocities in occlusions, we filter out 230 relevant cut-in scenarios from the 5,600 recorded lane changes in the highD dataset. We classify a cut-in as a lane change where a vehicle starts less than 100 meters in front of another vehicle in the destination lane. Since the speed limit in the dataset varies (or is even unlimited), we only consider scenarios where the velocities are between 110 and 135 $\mathrm{km\,h^{-1}}$ for the overtaking vehicle. Both vehicles must also be in the scenario 3.6 seconds before the lane change and 5.4 seconds after it. The following vehicle in the destination lane will be considered the ego vehicle. Any recorded vehicles behind the ego vehicle are removed.

B. Qualitative Example

In Fig. 5, we show a typical example where our proposed method makes a significant difference. The figure shows three snapshots, each with the proposed algorithm on top and the baseline at the bottom. The ego vehicle (in yellow) is being overtaken by a faster vehicle (in blue) which then occludes the view ahead of it. By tracking the occlusion, we conclude that only a small object (e.g., a motorcycle) can hide in the occluded area behind the overtaking vehicle (in the dark red region). However, with the baseline method, this hidden object may have a zero velocity. In Fig. 5, the effect of this can be seen by looking at the predicted occupied space (Def. 9) at the last time interval of the planned trajectory, i.e. $\hat{\mathcal{O}}_{[\tau+(N-1)\Delta t, \tau+N\Delta t]}$. This space is represented in red, and the area in a lighter shade of red represents space that is predicted occupied at the earlier time intervals of the planning horizon, but free at the end of the planning horizon, namely $\hat{\mathcal{O}}_{[\tau, \tau+(N-1)\Delta t]}$. At the initial time step, both methods give the same result. However, after 1 second of tracking, our method bounds the velocity in the occlusion and predicts a significantly smaller space to possibly be occupied at the end of the planning horizon.

In Fig. 6, we visualize our method's tracked set of possible states (projected on the xv-plane) for 20 consecutive time steps in the same scenario. The graph shows that 20 meters (in x) initially is occluded and may be occupied by a vehicle with a velocity between 0 and 135 $\mathrm{km\,h^{-1}}$ (37.5 $\mathrm{m\,s^{-1}}$). Eventually, the velocity in the occlusion gets a lower bound around 100 $\mathrm{km\,h^{-1}}$.

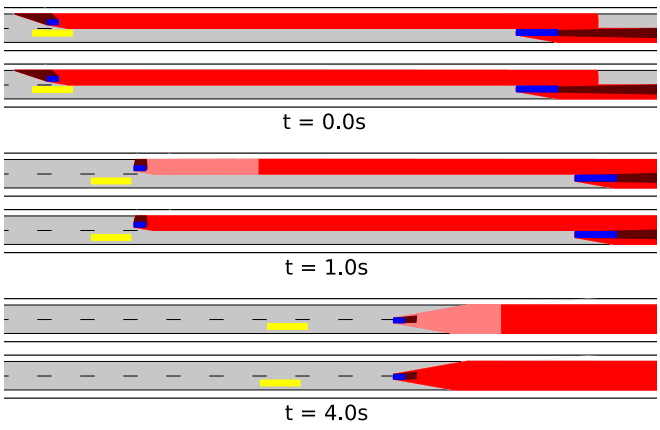

Fig. 5. The ego vehicle (in yellow) gets overtaken by another vehicle (in blue), causing an occlusion (in dark red). Using velocity tracking (examples on top), we reduce the predicted occupied space at the final time interval of our planning horizon (in red). The removed area (in light red) shall be avoided at earlier time intervals of the plan (following Def. 9).

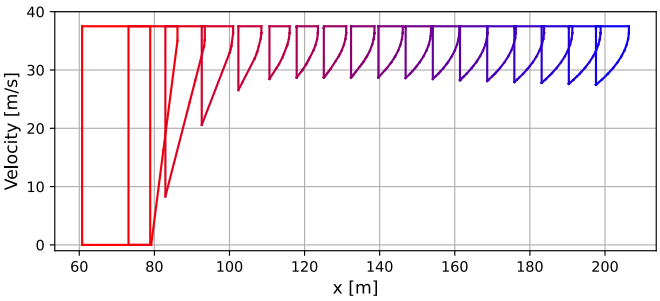

Fig. 6. Tracked set of possible velocities along the occlusion in x, visualized from $t = 0$ (in red) to $t = 3.6$ (in blue).

The effect on the motion planner can be seen in Fig. 7, showing the ego vehicle's velocity profiles. With our method, no speed reduction is needed to guarantee a collision-free trajectory. This is the same result as if there were no occlusions and the ego vehicle had ideal knowledge of the scene. With the baseline method, the planner is incapable of guaranteeing a collision-free trajectory due to considering the possibility of a stationary vehicle being in the occluded area. This causes the baseline method to initiate an emergency braking for 1 second until a safe distance is restored.

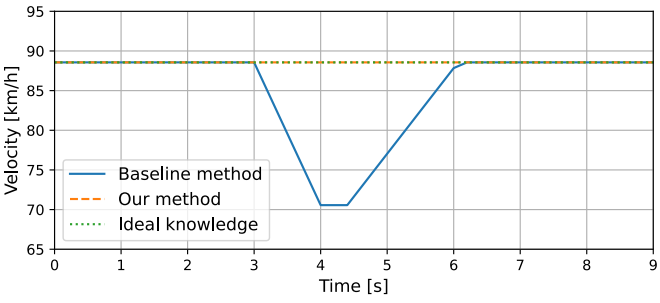

Fig. 7. Achieved velocity during the scenario using the two methods.

C. Quantitative Results

In Fig. 8, we present a comparison of the minimal speed reduction achieved with the two methods for the 230 evaluated cut-in scenarios. This 2D histogram visualizes how many scenarios have a certain speed reduction with each method. The baseline's speed reduction is plotted on the x-axis and our method's speed reduction is on the y-axis. In every scenario, our method matches or outperforms the baseline. Notably, a smaller speed reduction is needed with our method in almost 60% of the scenarios (137/230). In those, the average improvement is a 7.9 $\mathrm{km\,h^{-1}}$ higher minimal speed. In 15 of the scenarios, our method can avoid any speed reduction (similar to Fig. 7). For a comprehensive analysis and detailed discussion of these quantitative results, we direct the reader to the master's thesis complementing this work [55].

The average computational time required for the tracking of the set of all possible hidden traffic participants' states (Algorithm 1) was 0.146 seconds per time step on an Intel Xeon(R) Platinum 8358 CPU. With a time step of 0.2 seconds, the method is already capable of running in real-time, despite no parallelization.

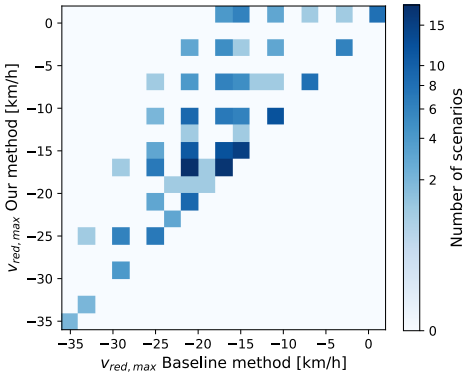

Fig. 8. 2D histogram of the speed achieved using the two methods.

V. Conclusions and Future Work

In this work, we present a novel method for tracking and establishing bounds on hidden traffic participants' velocities. This enables planning trajectories guaranteed to be collision-free, while still maintaining good performance, as shown in the many scenarios found in the highD dataset.

For future work, we aim to test the robustness and limitations of our proposed method using real sensor data in a real-time system. This will need an optimized implementation of the planner and the predictions in Algorithm 2, which was not prioritized in this work. Moreover, our method can be extended with more model abstractions. In [17], the authors suggest using a curvilinear coordinate system and a longitudinal abstraction to handle more general road geometries. They also propose an abstraction handling others' duty of care inspired by the Responsibility-Sensitive Safety model (RSS) [11]. With an algorithm to detect objects within the field of view, such an abstraction would prevent our method from considering hidden objects to follow other objects unrealistically close.

REFERENCES

[1] Technical Committee: ISO/TC 22/SC 33, "ISO 22733-1:2022 - Road vehicles — test method to evaluate the performance of autonomous emergency braking systems — part 1: Car-to-car," Sep 2022.

[2] Technical Committee: ISO/TC 22/SC 33, "ISO 19377:2017 Heavy commercial vehicles and buses — emergency braking on a defined path — test method for trajectory measurement," Nov 2017.

[3] Mercedes-Benz Group AG, "Certification for SAE level 3 system for U.S. market," Jan 2023.

[4] California Public Utilities Commission, "CPUC approves permits for cruise and waymo to charge fares for passenger service in San Francisco," August 2023.

[5] P. Koopman, *How safe is safe enough?: Measuring and predicting autonomous vehicle safety*. Amazon Digital Services LLC - Kdp, 2022.

[6] Technical Committee: ISO/TC 22/SC 32, "ISO/CD TS 5083 Road vehicles — safety for automated driving systems — design, verification and validation."

[7] M. S. Elli and J. Weast, "Towards a formal model for safe and scalable automated vehicle decision-making: A brief survey on responsibility-sensitive safety," *SAE International Journal of Connected and Automated Vehicles*, vol. 4, pp. 12–04–01–0002, Mar 2021.

[8] S. Maierhofer, P. Moosbrugger, and M. Althoff, "Formalization of Intersection Traffic Rules in Temporal Logic," in *2022 IEEE Intelligent Vehicles Symposium (IV)*, (Aachen, Germany), pp. 1135–1144, June 2022.

[9] N. Mehdipour, M. Althoff, R. D. Tebbens, and C. Belta, "Formal methods to comply with rules of the road in autonomous driving: State of the art and grand challenges," *Automatica*, vol. 152, p. 110692, Jun 2023.

[10] K. X. Cai, T. Phan-Minh, S.-J. Chung, and R. M. Murray, "Rules of the road: Formal guarantees for autonomous vehicles with behavioral contract design," *IEEE Transactions on Robotics*, p. 1–20, 2023.

[11] S. Shalev-Shwartz, S. Shammah, and A. Shashua, "On a formal model of safe and scalable self-driving cars," *arXiv:1708.06374 [cs, stat]*, Oct 2018. arXiv: 1708.06374.

[12] A. Censi, K. Slutsky, T. Wongpiromsarn, D. Yershov, S. Pendleton, J. Fu, and E. Frazzoli, "Liability, ethics, and culture-aware behavior specification using rulebooks," in *2019 International Conference on Robotics and Automation (ICRA)*, p. 8536–8542, May 2019.

[13] C.-I. Vasile, J. Tumova, S. Karaman, C. Belta, and D. Rus, "Minimum-violation scltl motion planning for mobility-on-demand," in *2017 IEEE International Conference on Robotics and Automation (ICRA)*, p. 1481–1488, May 2017.

[14] P. Karle, M. Geisslinger, J. Betz, and M. Lienkamp, "Scenario understanding and motion prediction for autonomous vehicles—review and comparison," *IEEE Transactions on Intelligent Transportation Systems*, vol. 23, p. 16962–16982, Oct 2022.

[15] A. Quintanar, R. Izquierdo, I. Parra, D. Fernández-Llorca, and M. A. Sotelo, "The prevention challenge: How good are humans predicting lane changes?," in *2020 IEEE Intelligent Vehicles Symposium (IV)*, p. 45–50, Oct 2020.

[16] M. Althoff and S. Magdici, "Set-Based Prediction of Traffic Participants on Arbitrary Road Networks," *IEEE Transactions on Intelligent Vehicles*, vol. 1, pp. 187–202, June 2016.

[17] M. Koschi and M. Althoff, "Set-based prediction of traffic participants considering occlusions and traffic rules," *IEEE Transactions on Intelligent Vehicles*, vol. 6, p. 249–265, Jun 2021.

[18] P. F. Orzechowski, A. Meyer, and M. Lauer, "Tackling occlusions & limited sensor range with set-based safety verification," in *2018 21st International Conference on Intelligent Transportation Systems (ITSC)*, p. 1729–1736, Nov 2018.

[19] S. K. Karanam, T. Duhautbout, R. Talj, V. Cherfaoui, F. Aioun, and F. Guillemard, "Virtual obstacle for a safe and comfortable approach to limited visibility situations in urban autonomous driving," in *2022 IEEE Intelligent Vehicles Symposium (IV)*, p. 909–914, Jun 2022.

[20] V. Narri, A. Alanwar, J. Mårtensson, C. Norén, L. Dal Col, and K. H. Johansson, "Set-membership estimation in shared situational awareness for automated vehicles in occluded scenarios," in *IEEE Intelligent Vehicles Symposium*, p. 385–392, 2021.

[21] M. Buchholz, J. Müller, M. Herrmann, J. Strohbeck, B. Völz, M. Maier, J. Paczia, O. Stein, H. Rehborn, and R.-W. Henn, "Handling occlusions in automated driving using a multiaccess edge computing server-based environment model from infrastructure sensors," *IEEE Intelligent Transportation Systems Magazine*, vol. 14, no. 3, p. 106–120, 2022.

[22] J. Müller, J. Strohbeck, M. Herrmann, and M. Buchholz, "Motion planning for connected automated vehicles at occluded intersections with infrastructure sensors," *IEEE Transactions on Intelligent Transportation Systems*, vol. 23, p. 17479–17490, Oct 2022.

[23] S. Li, K. Shu, C. Chen, and D. Cao, "Planning and decision-making for connected autonomous vehicles at road intersections: A review," *Chinese Journal of Mechanical Engineering*, vol. 34, p. 133, Dec 2021.

[24] W. Schwarting, J. Alonso-Mora, and D. Rus, "Planning and decision-making for autonomous vehicles," *Annual Review of Control, Robotics, and Autonomous Systems*, vol. 1, no. 1, p. 187–210, 2018.

[25] T. Nyberg, C. Pek, L. Dal Col, C. Norén, and J. Tumova, "Risk-aware motion planning for autonomous vehicles with safety specifications," in *2021 IEEE Intelligent Vehicles Symposium (IV)*, p. 1016–1023, Jul 2021.

[26] M. Geisslinger, F. Poszler, and M. Lienkamp, "An ethical trajectory planning algorithm for autonomous vehicles," *Nature Machine Intelligence*, vol. 5, p. 137–144, Feb 2023.

[27] C. van der Ploeg, R. Smit, A. Teerhuis, and E. Silvas, "Long horizon risk-averse motion planning: A model-predictive approach," in *2022 IEEE 25th International Conference on Intelligent Transportation Systems (ITSC)*, p. 1141–1148, Oct 2022.

[28] M. Koç, E. Yurtsever, K. Redmill, and U. Özgüner, "Pedestrian emergence estimation and occlusion-aware risk assessment for urban autonomous driving," in *2021 IEEE International Intelligent Transportation Systems Conference (ITSC)*, (Indianapolis, IN, USA), p. 292–297, IEEE Press, Sep 2021.

[29] D. Wang, W. Fu, Q. Song, and J. Zhou, "Potential risk assessment for safe driving of autonomous vehicles under occluded vision," *Scientific Reports*, vol. 12, p. 4981, Mar 2022.

[30] M. Naumann, H. Konigshof, M. Lauer, and C. Stiller, "Safe but not Overcautious Motion Planning under Occlusions and Limited Sensor Range," in *2019 IEEE Intelligent Vehicles Symposium (IV)*, (Paris, France), pp. 140–145, IEEE, June 2019.

[31] P. Schörner, D. Grimm, and J. M. Zöllner, "Towards multi-modal risk assessment," in *2022 International Conference on Electrical, Computer, Communications and Mechatronics Engineering (ICECCME)*, p. 1–7, Nov 2022.

[32] M.-Y. Yu, R. Vasudevan, and M. Johnson-Roberson, "Occlusion-Aware Risk Assessment for Autonomous Driving in Urban Environments," *IEEE Robotics and Automation Letters*, vol. 4, pp. 2235–2241, Apr. 2019.

[33] R. Poncelet, A. Verroust-Blondet, and F. Nashashibi, "Safe geometric speed planning approach for autonomous driving through occluded intersections," in *2020 16th International Conference on Control, Automation, Robotics and Vision (ICARCV)*, p. 393–399, Dec 2020.

[34] B. Gilhuly, A. Sadeghi, P. Yedmellat, K. Rezaee, and S. L. Smith, "Looking for trouble: Informative planning for safe trajectories with occlusions," in *2022 International Conference on Robotics and Automation (ICRA)*, p. 8985–8991, May 2022.

[35] P. Narksri, H. Darweesh, E. Takeuchi, Y. Ninomiya, and K. Takeda, "Occlusion-aware motion planning with visibility maximization via active lateral position adjustment," *IEEE Access*, vol. 10, p. 57759–57782, 2022.

[36] C. Hubmann, N. Quetschlich, J. Schulz, J. Bernhard, D. Althoff, and C. Stiller, "A POMDP Maneuver Planner For Occlusions in Urban Scenarios," in *2019 IEEE Intelligent Vehicles Symposium (IV)*, pp. 2172–2179, June 2019.

[37] X. Lin, J. Zhang, J. Shang, Y. Wang, H. Yu, and X. Zhang, "Decision making through occluded intersections for autonomous driving," in *2019 IEEE Intelligent Transportation Systems Conference (ITSC)*, p. 2449–2455, Oct 2019.

[38] C. Zhang, F. Steinhauser, G. Hinz, and A. Knoll, "Improved occlusion scenario coverage with a pomdp-based behavior planner for autonomous urban driving," in *2021 IEEE International Intelligent Transportation Systems Conference (ITSC)*, p. 593–600, Sep 2021.

[39] Z. Zhang and J. Fisac, "Safe occlusion-aware autonomous driving via game-theoretic active perception," in *Robotics: Science and Systems XVII*, Robotics: Science and Systems Foundation, Jul 2021.

[40] M. Kahn, A. Sarkar, and K. Czarnecki, "I know you can't see me: Dynamic occlusion-aware safety validation of strategic planners for autonomous vehicles using hypergames," in *2022 International Conference on Robotics and Automation (ICRA)*, p. 11202–11208, May 2022.

[41] D. Isele, R. Rahimi, A. Cosgun, K. Subramanian, and K. Fujimura, "Navigating Occluded Intersections with Autonomous Vehicles using Deep Reinforcement Learning," in *2018 IEEE International Conference on Robotics and Automation (ICRA)*, (Brisbane, Australia), pp. 2034–2039, May 2017.

[42] F. Christianos, P. Karkus, B. Ivanovic, S. V. Albrecht, and M. Pavone, "Planning with occluded traffic agents using bi-level variational occlusion models," in *2023 IEEE International Conference on Robotics and Automation (ICRA)*, p. 5558–5565, May 2023.

[43] J. M. G. Sánchez, T. Nyberg, C. Pek, J. Tumova, and M. Törngren, "Foresee the unseen: Sequential reasoning about hidden obstacles for safe driving," in *2022 IEEE Intelligent Vehicles Symposium (IV)*, p. 255–264, Jun 2022.

[44] Y. Nager, A. Censi, and E. Frazzoli, "What lies in the shadows? safe and computation-aware motion planning for autonomous vehicles using intent-aware dynamic shadow regions," in *2019 International Conference on Robotics and Automation (ICRA)*, p. 5800–5806, May 2019.

[45] L. Wang, C. Burger, and C. Stiller, "Reasoning about potential hidden traffic participants by tracking occluded areas," in *2021 IEEE International Intelligent Transportation Systems Conference (ITSC)*, p. 157–163, Sep 2021.

[46] G. Neel and S. Saripalli, "Improving bounds on occluded vehicle states for use in safe motion planning," in *2020 IEEE International Symposium on Safety, Security, and Rescue Robotics (SSRR)*, p. 268–275, Nov 2020.

[47] R. Rajamani, *Vehicle Dynamics and Control*. Mechanical Engineering Series, Boston, MA: Springer US, 2012.

[48] M. Althoff, *Reachability Analysis and its Application to the Safety Assessment of Autonomous Cars*. Dissertation, TUM, Munchen, Feb. 2010.

[49] S. Haddad and A. Halder, "The convex geometry of integrator reach sets," in *2020 American Control Conference (ACC)*, pp. 4466–4471, 2020.

[50] R. Krajewski, J. Bock, L. Kloeker, and L. Eckstein, "The highd dataset: A drone dataset of naturalistic vehicle trajectories on german highways for validation of highly automated driving systems," in *2018 21st International Conference on Intelligent Transportation Systems (ITSC)*, p. 2118–2125, Nov 2018.

[51] M. Althoff, M. Koschi, and S. Manzinger, "Commonroad: Composable benchmarks for motion planning on roads," in *2017 IEEE Intelligent Vehicles Symposium (IV)*, p. 719–726, Jun 2017.

[52] T. C. Project, "CGAL - the computational geometry algorithms library," 2023.

[53] S. Gillies, "Shapely: Manipulation and analysis of geometric objects," 2007.

[54] C. Pek, V. Rusinov, S. Manzinger, M. C. Üste, and M. Althoff, "Commonroad drivability checker: Simplifying the development and validation of motion planning algorithms," in *IEEE Intelligent Vehicles Symposium (IV)*, p. 1013–1020, 2020.

[55] J. van Haastregt, "Occlusion-aware autonomous highway driving : Tracking safe velocity bounds on potential hidden traffic for improved trajectory planning," Master's thesis, KTH, School of Electrical Engineering and Computer Science (EECS), 2023.